Effects of compositional disorder on phonons in layered semiconductor microstructures

F. Bechstedt, H. Gerecke, and H. Grille
Friedrich-Schiller-Universität, Max-Wien-Platz, O-6900 Jena, Germany
(Received 18 September 1992; revised manuscript received 20 January 1993)

The random-element-isodisplacement (REI) model developed originally to describe zone-center optical phonons in ternary mixed crystals is generalized. Starting from a certain configurational average that defines an average composition within an atomic or a molecule layer perpendicular to a given growth direction, we derive equations of motion for the averaged atomic displacements and the correlation of fluctuations in composition and displacements. The long-range macroscopic electric field is included fully. We show that phonons with arbitrary wave vectors can be studied for the configurationally averaged layered system. The density of states resulting from this model is compared with that from a numerical simulation of the full disorder using extended supercells. The comparison shows that only disorder-induced broadening effects are neglected within the generalized REI model. The power of the model is explicitly demonstrated for pure mass disorder in $(GaAs)_{N_1}(Ga_{1-x}Al_xAs)_{N_2}(001)$ superlattices. Different cases of cation interdiffusion at the interfaces of $(GaAs)_{N_1}(AlAs)_{N_2}$ structures and the influence of barrier composition are studied.

I. INTRODUCTION

Ternary mixed semiconductor crystals $A_{1-x}B_xC$ are widely used to produce lattice-matched heterostructures and superlattices and to tailor their physical properties with the composition x in the different material layers. Recent progress in monolayer control of epitaxial techniques has allowed the growth of ultrathin superlattices with periods of a few atomic planes. Nevertheless, the interfaces between two adjacent materials, e.g., $AC/A_{1-x}B_xC$, are far from ideal. There exists a long-range interface roughness related to step-bounded island parallel to the nominal interfaces and short-range interface roughness accompanying atomic diffusion normal to the interfaces. Despite the perfection of the grown material layers a further problem is due to the composition in these layers itself. The composition not only changes physical properties such as the quantum-mechanical confinement of electrons and phonon modes, it is always accompanied with effects of compositional disorder.

In recent years much interest has been devoted to the basic understanding of the modification of the vibrational properties of layered materials compared to the corresponding ideal structures and the underlying bulk crystals.[1-3] In this respect $Ga_{1-x}Al_xAs$ alloys are studied as prototypical materials. They are usually arranged in $(GaAs)_{N_1}(Ga_{1-x}Al_xAs)_{N_2}(001)$ superlattices with varying composition x and numbers of molecule layers N_1 and N_2 grown along a cubic axis. The corresponding material layers are lattice matched. The optical bands of GaAs and AlAs do not overlap, so in a layered structure formed from these materials the optical modes are well confined within the parent crystal slab. The different materials differ only by the cations from each other.

There are several reasons for studying the vibrational properties of heterostructures composed by $Ga_{1-x}Al_xAs$ slabs with different Al concentrations x: (i) to understand the effects on the dynamics of cation interdiffusion at GaAs/AlAs interfaces, (ii) the possibility of folding back the optical dispersion relations for bulk homogeneous alloys, and (iii) to study the interplay between structures activated by the local compositional disorder and those induced by the superstructure ordering. Large discrepancies between theoretical expectations[4,5] and experiments[6-10] are found for the $N/2=N_1=N_2$ dependence of the first confined longitudinal-optical-phonon peak LO1 in ultrathin $(GaAs)_{N/2}(AlAs)_{N/2}(001)$ superlattices ($N \leq 8$) since the very first studies. The discrepancies can be largely explained by the effects of interface broadening.[11-14] However, it appears that the actual details of the interface roughness are rather complicated. Besides the influence of the cation interdiffusion the frequency shift there may also be effects of the interface roughness due to the in-plane terraces.[15,16] Raman measurements[17,18] have shown the frequencies of the confined LO phonons to be a sensitive probe of the latter, which especially occurs at the inverse interface, i.e., GaAs on AlAs. Now also little is known about the effect of interface broadening on the confined TOn modes.[13,15]

The composition x in the $Ga_{1-x}Al_xAs$ barrier layers and the related local compositional disorder also influence the confinement of the LOn and TOn modes. Very recently the first observation of a confined-to-propagating transition of LO phonons in $(GaAs)_{N_1}(Ga_{1-x}Al_xAs)_{N_2}(001)$ superlattices is reported.[19] In dependence on the Al content x the decay length of the GaAs-like phonons exhibits rapid changes versus the barrier thickness $\sim N_2$. Such a tendency is seemingly also observed when studying the dispersive character of the optical phonons in $(Ga_{1-x}Al_xAs)_{N_1}(AlAs)_{N_2}$ (001) superlattices.[20] For any given composition x, the alloy exhibits a two-mode behavior[21-27] in the optical branch region with frequencies somewhat below the pure GaAs or AlAs optical phonons. Therefore confinement can occur for the highest GaAs-like (AlAs-like) modes in

GaAs/$Ga_{1-x}Al_xAs$ ($Ga_{1-x}Al_xAs$/AlAs) systems. However, it depends on x and even vanishes when the corresponding bulk dispersion branches overlap energetically.

An early theoretical study of the effect of interface roughness was based on a linear-chain model[28] with an alloy potential added at the interface sites. The potential was obtained from a bulk calculation within the coherent-potential approximation (CPA). It therefore neglects effects of the layered structure. This type of model calculation is later extended also to three-dimensional lattice-dynamic calculations.[11,20,29] More recently the problem of interface disorder has been tackled by the direct diagonalization of the lattice-dynamical problem for sufficiently large supercells with stochastic occupation of the cation sites.[5,14,30] The appearing force constants have been derived by a fitting procedure from results of *ab initio* calculations. This type of calculation satisfactorily reproduces the experimental findings for the interface-disorder influence. Nevertheless, the enormous computational effort required reduces the versatility of the approach. More strictly speaking, its application is limited to ultrathin samples. Therefore approximate descriptions to determine the disorder-induced phonon self-energies are further necessary. An important class in this respect contains mean-field methods. Besides the CPA, which has recently been applied to the full system of GaAs/AlAs(001) superlattices with disordered interfaces,[12] such a method is the averaged-t-matrix approximation (ATA). The dielectric function and the Raman intensity are calculated within ATA applying a bond-charge model to the lattice dynamics and restricting to mass-defect approximation.[31]

Another class of approximations starts from general features in the phonon structure in the mixed crystals $A_{1-x}B_xC$ on the base of many III-V and II-VI semiconductors. For instance, experimental[25,32] and theoretical[27] findings indicate that Raman- and infrared-active phonons in $Ga_{1-x}Al_xAs$ alloys have well-defined momenta and only a small disorder-induced line broadening. Raman studies of the corresponding superlattices support this picture.[20] Alloys of this type, therefore, can be treated as pseudolinear materials, even if no neutron diffraction data exist which confirm the existence of defined phonon-dispersion relations. Starting from the assumption of negligible broadening of phonon states a rigorous simplification of the theoretical description can be reached. The most famous model for $A_{1-x}B_xC$ alloys in this respect is the random-element-isodisplacement (REI) model of Chen, Shockley, and Pearson,[21] that has been later modified by Chang and Mitra[33] to include the polarization field. The model explains the transition from one-mode to two-mode behavior for transverse- and longitudinal-optical phonons in mixed crystals. Unfortunately it is restricted to the description of long-wavelength phonons. The fundamental idea of the REI model is that A and B atoms are randomly distributed on the corresponding sublattice and that all atoms occupying one sublattice vibrate in phase and with identical amplitudes. The assumption of isodisplacement is exactly true for zone-center vibrations in ordered binary crystals. Its extension to mixed ternary crystals therefore requires the introduction of pseudounit cells. The successful explanation of the dependence of zone-center optical-phonon energies on the composition parameter x of alloys[25,33] as well as the electron-phonon interaction[34] gives some hope of extending the REI model to more complex structures like superlattices with similar success. Promising attempts[13,35] in this direction have been done using a one-dimensional model for phonons propagating along the superlattice axis and omitting the details of the long-range electric field.

In this paper we describe the details of a theory for phonons in layered semiconductor structures on the base of $A_{1-x}B_xC$ materials with a certain concentration profile x along the growth direction. The theory includes the full dynamical matrix of the system, i.e., also the Coulomb part reflecting the long-range macroscopic electric field, and should not be restricted to long-wavelength modes and certain phonon propagation directions. The approximations made within the theory are especially valid for $(AC)_{N_1}(A_{1-x}B_xC)_{N_2}$ superlattices grown in [001] direction with arbitrary composition profiles in the interface region between AC and $A_{1-x}B_xC$ ($0<x\leq 1$). As a limiting case a REI model for the zone-center optical phonons of (001) superlattices should be contained in the theory. In Sec. II the equations of motion of the atoms in the system are configurationally averaged in such a way that for each atomic layer perpendicular to the growth direction an average concentration of B atoms can be introduced. The hierarchy of equations is decoupled by a one-site approximation of higher correlation functions of composition-induced fluctuations. As a result a generalized REI model for arbitrary lattice vibrations appears. In Sec. III the lattice-dynamical problem is specified to (001) superlattices with a certain composition profile. With regard to the GaAs/$Ga_{1-x}Al_xAs$ system the dynamical matrix is simplified assuming pure mass disorder and a reasonable description of elastic and electric forces in the framework of the Born-Huang model. Explicit results for these superlattices are obtained for densities of states, frequencies, and spectral weights. The densities of states are compared with results from an exact calculation using sufficiently large supercells which realize all configurations in the system. Mainly two effects are discussed in Sec. IV, the influence of alloying in the $Ga_{1-x}Al_xAs$ barrier layers and the influence of interface broadening on the vibrational properties. Finally, a summary is given in Sec. V.

II. BASIC EQUATIONS

A. Configuration average

We consider a layered semiconductor structure consisting of materials $A_{1-x}B_xC$ of different compositions x and with interfaces which can be represented by certain composition profiles. Hence one has to deal with the interplay of three important effects, the layered structure due to the growth process, the compositional disorder in the material layers prepared by a ternary mixed crystal, and the compositional disorder related to the atom

interdiffusion at the $A_{1-y}B_yC/A_{1-x}B_xC$ interfaces. On the other hand, the atomic sites are considered to be completely ordered in correspondence with the crystal structures of the grown material layers and eventually the substrate in the case of strained-layer systems. Modeling the layered and alloyed system we characterize the atomic sites $\mathbf{R}_{nml}$ in the regular lattice by a sublattice index $n=1$ or 2, a layer index m labeling the atomic layers perpendicular to the growth direction of the structure, and an index l running over all atomic sites of type $n=1$ or 2 within one atomic layer m. The sublattice $n=1$ is assumed to be randomly occupied by A atoms with the layer-dependent concentration $(1-x_m)$ and B atoms with the concentration x_m. The sublattice $n=2$ remains completely occupied with C atoms. The displacements of atoms at the site $\mathbf{R}_{nml}$ obey equations of motion of the type

$$\omega^2 M(nml)u_\alpha(nml) = \sum_{n',m',l'}\sum_{\alpha'} F_{\alpha\alpha'}(nml,n'm'l')u_{\alpha'}(n'm'l') , \quad (1)$$

with $u_\alpha(nml)$ as the αth Cartesian component. The matrix of the force constants represents both the short-range elastic forces, taken within the harmonic approximation, and the long-range electric forces proportional to the square of the effective charges $e(nml)$ of the atoms.

We assume that the force constants $F_{\alpha\alpha'}(nml,n'm'l')$, the effective charges $e(nml)$, and the masses $M(nml)$ depend only on the occupation of the $\mathbf{R}_{nml}$ and $\mathbf{R}_{n'm'l'}$ but not on the surroundings. Introducing occupation numbers ($j=A,B,C$)

$$\eta_j(nml)=\begin{cases}1 & \text{if an atom of kind } j \text{ is placed on site } \mathbf{R}_{nml}\\ 0 & \text{otherwise} ,\end{cases} \quad (2)$$

with the properties

$$\eta_j(nml)\eta_{j'}(nml)=\eta_j(nml)\delta_{jj'} ,$$
$$\sum_j \eta_j(nml)=1 , \quad (3)$$
$$\sum_l \eta_j(nml)=c_j(m)N(nm) ,$$

where $c_j(m)$ denotes the concentration of atoms of the jth species in the mth layer. It holds $c_A(m)=1-x_m$, $c_B(m)=x_m$, and $c_C(m)=1$. We mention that the number of sites of the sublattice n in the mth layer, $N(nm)=\sum_l$, may be zero for one atomic species n, e.g., for growth directions parallel [111] and [001]. Using the occupation numbers defined in Eq. (2), the masses and elements of the force-constant matrix appearing in the set of equations (1) may be expressed as ($j=A,B,C$)

$$M(nml)=\sum_j \eta_j(nml)M_j(n) ,$$
$$F_{\alpha\alpha'}(nml,n'm'l')=\sum_{j,j'}\eta_j(nml)F^{jj'}_{\alpha\alpha'}(nml-n'm'l')\times\eta_{j'}(n'm'l') . \quad (4)$$

Here we define $M_A(1)=M_A$, $M_B(1)=M_B$, $M_C(1)=0$, $M_A(2)=0$, $M_B(2)=0$, and $M_C(2)=M_C$ with M_A, M_B, and M_C as the masses of the A, B, and C atoms, respectively. Since the force constants are governed only by the two atoms connected by it, we have assumed $F^{jj'}_{\alpha\alpha'}(nml,n'm'l')=F^{jj'}_{\alpha\alpha'}(nml-n'm'l')$ in accordance with the restriction to compositional disorder.

For a given microscopic configuration, i.e., fixed distribution of atoms A and B over the corresponding sublattice sites, in a certain volume V containing N_V atoms the set of $3N_V$ linear homogeneous equations in the $3N_V$ variables $u_\alpha(nml)$ can be solved giving $3N_V$ eigenfrequencies and eigenmodes. However, the basic problem in dealing with disordered solids is that the microscopic configuration of a given sample is unknown. Therefore the conception of the ensemble or configuration average $\langle\ \rangle_c$ of physically observable quantities was developed, where an ensemble consists of elements corresponding to all possible atomic configurations which cannot be distinguished macroscopically.[36] We apply two different methods performing the configuration average. For the purpose of comparison we perform the average numerically, at least for a very simple matrix $F_{\alpha\alpha'}(nml,n'm'l')$ of force constants. The considered volume V is divided into large supercells.[27] The size of the supercells necessary to simulate the effects of compositional disorder is chosen large enough so that it is already representative for a whole ensemble of systems, i.e., the selected supercells at hand are assumed to be self-averaging.

The second method aims at the possibility of an analytical performance of the configuration average. This average acts on the occupation numbers since they contain the statistics of the atoms. Thus as a result of the average procedure one has to deal with expectation values like $\langle\eta_j(nml)\rangle_c$, $\langle\eta_j(nml)\eta_{j'}(n'm'l')\rangle_c$, etc. that characterize the occupation probabilities of one, two, etc. sites of the lattice if $nml\neq n'm'l'$. In particular, it holds that

$$\langle\eta_j(nml)\rangle_c=c_j(m) . \quad (5)$$

Furthermore, we introduce averaged atomic displacement fields according to

$$v_{j\alpha}(nml)=\frac{\langle\eta_j(nml)u_\alpha(nml)\rangle_c}{\langle\eta_j(nml)\rangle_c} . \quad (6)$$

B. Averaged equations of motion

We start from Eq. (1). Replacing in this equation the masses and the coupling constants by means of the definitions (4) and multiplying the resulting equation with $\eta_j(nml)$ we obtain with Eqs. (3) and (6) and after configuration average

$$\sum_{\alpha'} \{\omega^2 M_j(n)\delta_{\alpha\alpha'} - F^{jj}_{\alpha\alpha'}(0)\} v_{j\alpha'}(nml) = \sum_{\alpha',j'} \sum_{n',m',l'}{}' F^{jj'}_{\alpha\alpha'}(nml - n'm'l') c_{j'}(m') \{v_{j'\alpha'}(n'm'l') + w_{jj'\alpha'}(nml|n'm'l')\} , \quad (7)$$

where the correlation function

$$w_{jj'\alpha'}(nml|n'm'l') = \frac{\langle \Delta\eta_j(nml)\Delta[\eta_{j'}(n'm'l')u_{\alpha'}(n'm'l')]\rangle_c}{c_j(m)c_{j'}(m')} \quad (8)$$

of fluctuations $\Delta O = O - \langle O \rangle_c$ around configurationally averaged values is introduced. The prime at the $n'm'l'$ sum indicates that the same site $\mathbf{R}_{nml}$ has to be excluded. The correlation functions of fluctuations in the site occupation and in the weighted displacement fields appearing on the right-hand side of Eq. (7) describe forces acting on the atoms in addition to those already present in the virtual-crystal approximation (VCA). That means, taking into account certain approaches for these correlation functions, approximations such as the REI model, ATA, or CPA can be derived. For a detailed discussion of the relations and discrepancies between the different approximations for the treatment of compositional disorder, the reader is referred to Ref. 36.

In the following we generalize the conventional REI model.[21,33,36] For this purpose we derive an additional equation of motion for the correlation function (8) from Eq. (1). Using the same procedure as in the derivation of Eq. (7) we find

$$\sum_{\alpha''} \{\omega^2 M_{j'}(n')\delta_{\alpha'\alpha''} - F^{j'j'}_{\alpha'\alpha''}(0)\} w_{jj'\alpha''}(nml|n'm'l') = \sum_{\alpha'',j''} \sum_{n'',m'',l''}{}' F^{j'j''}_{\alpha'\alpha''}(n'm'l' - n''m''l'') \frac{\langle \Delta\eta_j(nml)\Delta[\eta_{j'}(n'm'l')\eta_{j''}(n''m''l'')u_{\alpha''}(n''m''l'')]\rangle_c}{c_j(m)c_{j'}(m')} . \quad (9)$$

A correlation function including three occupation numbers appears on the right-hand side of Eq. (9). A hierarchy of connected equations of correlation functions with one, two, three, etc. atomic sites can be derived. We decouple the hierarchy by a single-site approximation $n''m''l'' = nml$. The new correlation function in Eq. (9) can be directly calculated using Eqs. (5) and (6). It follows that ($nml \neq n'm'l'$)

$$\langle \Delta\eta_j(nml)\Delta[\eta_{j'}(n'm'l')\eta_{j''}(nml)u_{\alpha''}(nml)]\rangle_c = [\delta_{jj''} - c_j(m)]c_{j'}(m')c_{j''}(m)\{v_{j''\alpha''}(nml) + w_{j'j''\alpha''}(n'm'l'|nml)\} . \quad (10)$$

Together with the approximate expression (10) Eqs. (7) and (9) represent a finite system. Nevertheless, it is convenient to simplify the set of equations of motion by a first-nearest-neighbor approximation. We neglect all long-range correlations in Eq. (7) by setting $\mathbf{R}_{n'm'l'} = \mathbf{R}_{nml} - (-1)^n \tau_i$ ($i = 1,2,3,\ldots$ number of nearest neighbors). For the tetrahedrally coordinated materials, which are the typical materials manufacturing layered semiconductor microstructures, there are four neighbors ($i = 1,2,3,4$). In unstrained IV-IV, III-V, and II-VI compounds the four tetrahedron vectors defining the nearest-neighbor positions are $\tau_1 = (a_0/4)(1,1,1)$, $\tau_2 = (a_0/4)(1,-1,-1)$, $\tau_3 = (a_0/4)(-1,1,-1)$, and $\tau_4 = (a_0/4)(-1,-1,1)$ with a_0 as the bulk lattice constant. Together with the fact that the occupation of sublattice 2 is not random, i.e., $\Delta\eta_j(2ml) = 0$, all correlations containing displacements in sublattice 1 vanish. It holds that $w_{jj'\alpha'}(nml|n'm'l') = \delta_{n1}\delta_{n'2}\delta_{j'C} w_{jC\alpha'}(1ml|2m'l')$ in Eq. (7). As a consequence of $j' = C$ the correlation function disappears on the right-hand side of Eq. (10). The physical meaning of the resulting modifications of Eqs. (9) is obvious. Formally expressing the correlators of fluctuations by means of these equations by the displacements of A and B atoms additional forces in the equations of motion (7) of the A and B atoms appear. One finds that the additional forces due to the nearest-neighbor correlations become frequency-dependent force constants as a generalization of the common REI model.[21,33,36] This frequency dependence of the additional impurity force constants is important for the validity of the sum rules. The additional Eq. (9) for the correlation functions gives rise to new modes, the so-called disorder-activated transverse-acoustic (DATA) or disorder-activated longitudinal-acoustic (DALA) modes[26,36] that are related to acoustic phonons from the zone edge of the underlying binary crystals.

The system of the averaged equations of motion (7) and (9) can be solved when the force constants $F^{jj'}_{\alpha\alpha'}(nml - n'm'l')$ are specified. For the N_V atomic sites in the volume V the $3N_V$ linear homogeneous equations (1) give $3N_V$ orthonormalized normal coordinates with $3N_V$ eigenfrequencies. Compared with the solutions for a certain microscopic configuration one obtains twice the number $3N_V$ of eigenmodes required from the system of averaged equations. That means that spectral weights of these modes are in general smaller than 1. Approximate expressions for these spectral weights are given in Eqs. (22) and (23).

III. SPECIFICATIONS: (001) SUPERLATTICES

A. Geometry

We consider superlattices grown in [001] direction. For this direction the atomic layers are in a distance of $a_0/4$. They are only occupied by atomic sites of either sublattice 1 or 2. That means there is an alternating arrangement of atomic layers formed by A and B or C atoms. We assume that within one superlattice elementa-

ry cell there are N double (or molecule) layers. On the average each of the double layers s ($s=1,\ldots,N$) consists of an $A_{1-x_s}B_{x_s}C$ ternary compound where the average mole fractions x_s of the B atoms define an arbitrary concentration profile within one superlattice elementary cell. The total layered structure shows a periodicity of all configurationally averaged physical observables according to $m=\kappa N+s$ where κ is an integer number. A corresponding bulk ternary mixed crystal can be represented by $N=1$.

Introducing the Bravais lattice $\{\mathbf{R}\}$ of the superlattice and the atomic basis $\mathbf{r}_s+\tau_1\delta_{n2}$ ($s=1,\ldots,N$) in the superlattice elementary cell all atomic sites in the layered structure can be represented as

$$\mathbf{R}_{nml}\hat{=}\mathbf{R}+\mathbf{r}_s+\tau_1\delta_{n2}\ , \tag{11}$$

where $\mathbf{r}_s$ are the positions of the A or B atoms and τ_1 describes the connecting vector of such an A or B atom to a nearest-neighbor C atom in a neighboring atomic layer. In unstrained superlattices made from tetrahedrally coordinated materials τ_1 represents a tetrahedron vector.

The totality of vectors in the reciprocal Bravais lattice $\{\mathbf{G}\}$ and the vectors $\mathbf{Q}$ from the Brillouin zone of the superlattice span the reciprocal space. Starting from the translational symmetry of all configurationally averaged quantities Fourier transformations are possible. We write, with Eq. (11) and the number N_s of superlattice elementary cells in the volume V,

$$v_{j\alpha}(\mathbf{R}+\mathbf{r}_s+\tau_1\delta_{n2}) = \sum_{\mathbf{Q}} e^{i\mathbf{Q}\cdot\mathbf{R}}\frac{1}{[M_j(n)c_j(s)]^{1/2}}e_{j\alpha}(sn|\mathbf{Q})\ . \tag{12}$$

The corresponding equations for the correlation of the fluctuations are ($j=A,B$)

$$w_{jC\alpha}(\mathbf{R}+\mathbf{r}_s|\mathbf{R}+\mathbf{r}_s+\tau_i) = \sum_{\mathbf{Q}} e^{i\mathbf{Q}\cdot\mathbf{R}}\left[\frac{1-c_j(s)}{4M_Cc_j(s)}\right]^{1/2}h_{j\alpha}(si|\mathbf{Q})\ . \tag{13}$$

Here the atomic concentrations are specified to be $c_A(s)=1-x_s$, $c_B(s)=x_s$, and $c_C(s)=1$.

As in the common REI model[21,33,36] we assume also in the generalized REI model that the phonon modes in the averaged system have a pronounced dispersive character and, therefore, can be characterized by wave vectors $\mathbf{Q}$ from the superlattice Brillouin zone (BZ). Then the equations of motion (7) and (9) change over into a set of $12N$ coupled homogeneous algebraic equations for each wave vector $\mathbf{Q}$. Because of the two different atoms A and B and the correlator of the fluctuations the number of equations is doubled compared to the case of a well-ordered superlattice.

B. Mass approximation and Born-Huang model

For a given matrix of force constants the equations of motion can be immediately solved. In the following we will demonstrate the solution for a simplified model that gives the most important features for systems like $Ga_{1-x}Al_xAs$. The most important difference in the vibrations of GaAs and AlAs results from the different cation masses. The so-called mass approximation,[14,18,23] in which for both materials the same matrix of force constants is used, gives phonon-dispersion relations practically indistinguishable from the real ones in the acoustical and the transverse-optic regions, while they differ by less than 10 cm^{-1} in the LO region. Since we are not interested in the details of the phonon structure but more in the influence of the concentration profile versus a superlattice elementary cell, we further simplify the matrix of force constants.

We apply the Born-Huang model.[37,38] In this model the elastic forces are restricted only to nearest-neighbor interaction with a force constant $f/4$, whereas the Coulomb force acting on the ions with charges e^* (A and B atoms) and $-e^*$ (C atoms) are taken into account in the framework of the macroscopic electric field. The force-constant matrix can be written as[38,39]

$$\begin{aligned} F^{jj'}_{\alpha\alpha'}(\mathbf{r}) &= E^{jj'}_{\alpha\alpha'}(\mathbf{r})+C^{jj'}_{\alpha\alpha'}(\mathbf{r})\ , \\ E^{jj'}_{\alpha\alpha'}(\mathbf{r}) &= \delta_{\alpha\alpha'}\tfrac{1}{4}f\sum_{i=1}^{4}[\delta_{\mathbf{r},0}-\delta_{\mathbf{r},\tau_i}-\delta_{\mathbf{r},-\tau_i}]\ , \\ C^{jj'}_{\alpha\alpha'}(\mathbf{r}) &= \hat{f}\frac{1}{N_sN}\sum_{\mathbf{Q},\mathbf{G}}\frac{(\mathbf{Q}+\mathbf{G})_\alpha(\mathbf{Q}+\mathbf{G})_{\alpha'}}{|\mathbf{Q}+\mathbf{G}|^2} \\ &\quad\times\Omega_{jj'}(\mathbf{Q}+\mathbf{G})e^{i(\mathbf{Q}+\mathbf{G})\cdot\mathbf{r}} \\ &\quad(\mathbf{Q}+\mathbf{G}\in\text{bulk BZ})\ , \end{aligned} \tag{14}$$

where the Coulomb force constant

$$\hat{f}=\frac{16\pi e^{*2}}{a_0^3} \tag{15}$$

and the structure factors

$$\begin{aligned} \Omega_{jj'}(\mathbf{Q}+\mathbf{G}) &= \delta_{jj'}+\delta_{jA}\delta_{j'B}+\delta_{jB}\delta_{j'A} \\ &\quad-(\delta_{jA}+\delta_{jB})\delta_{j'C}S(\mathbf{Q}+\mathbf{G}) \\ &\quad-\delta_{jC}(\delta_{j'A}+\delta_{j'B})S^*(\mathbf{Q}+\mathbf{G})\ , \\ S(\mathbf{Q}+\mathbf{G}) &= \tfrac{1}{4}\sum_{i=1}^{4}\exp[i(\mathbf{Q}+\mathbf{G})\cdot\tau_i] \end{aligned} \tag{16}$$

of the superlattice and the underlying bulk zinc-blende structure are introduced. We mention that the Fourier components contributing to the matrix of Coulomb forces are restricted to wave vectors from the Brillouin zone of the zinc-blende structure. That is a consequence of the spatial average during the transition from the microscopic to the macroscopic electrodynamics.

C. Long-wavelength limit

The most important phonons for Raman scattering and infrared optical measurements are such with wave vectors from the center of the superlattice Brillouin zone. The long-wavelength limit of the elastic part is trivial. The Coulomb part decays into a sum of analytic ($\mathbf{G}\neq 0$) and nonanalytic ($\mathbf{G}=0$) contributions.[37,40] In the case of

superlattices the **G** sum can be performed.[38,39] Identifying the growth axis of the superlattice with the z direction of the Cartesian coordinate system and turning the two other axes so that the phonon propagation direction $\mathbf{Q}/|\mathbf{Q}|=(0,\sin\theta,\cos\theta)$ can only be related to the angle θ between the propagation direction and the growth axis, the total matrix of force constants can be analytically expressed as ($N>1$)

$$E^{jj'}_{\alpha\alpha'}(sn,s'n'|\theta)+C^{jj'}_{\alpha\alpha'}(sn,s'n'|\theta)=(\delta_{\alpha\alpha'}f+\delta_{\alpha z}\delta_{\alpha' z}\hat{f})$$
$$\times\{[(\delta_{jA}+\delta_{jB})(\delta_{j'A}+\delta_{j'B})+\delta_{jC}\delta_{j'C}]\delta_{ss'}\delta_{nn'}-[(\delta_{jA}+\delta_{jB})\delta_{j'C}+\delta_{jC}(\delta_{j'A}+\delta_{j'B})]$$
$$\times[\tfrac{1}{2}(\delta_{ss'}+\delta_{ss'+1})\delta_{n1}\delta_{n'2}+\tfrac{1}{2}(\delta_{ss'}+\delta_{ss'-1})\delta_{n2}\delta_{n'1}]\}$$
$$+\hat{f}(\delta_{jA}+\delta_{jB}-\delta_{jC})(\delta_{j'A}+\delta_{j'B}-\delta_{j'C})\frac{1}{N}A_{\alpha\alpha'}(\theta)\ , \tag{17}$$

with the rotation matrix[41–43]

$$A_{\alpha\alpha'}(\theta)=\frac{Q_\alpha Q_{\alpha'}}{|\mathbf{Q}|^2}-\delta_{\alpha z}\delta_{\alpha' z}=\sin\theta[\sin\theta(\delta_{\alpha y}\delta_{\alpha' y}-\delta_{\alpha z}\delta_{\alpha' z})+\cos\theta(\delta_{\alpha y}\delta_{\alpha' z}+\delta_{\alpha z}\delta_{\alpha' y})]\ . \tag{18}$$

For phonons with $|\mathbf{Q}|=0$ but a certain propagation direction with an angle θ to the growth axis one derives from Eqs. (7) and (9), using the real-space and Fourier-space representations (14) and (17) of the force-constant matrix, the following equations of motion [$jn=A1,B1,C2$; $c_A(s)=1-x_s$, $c_B(s)=x_s$, $c_C(s)=1$]:

$$\left[\omega^2-\frac{1-c_j(s)}{M_j}(f+\tfrac{1}{3}\hat{f})\right]e_{j\alpha}(sn|\theta)+(-1)^n\left[\frac{c_j(s)}{M_j}\right]^{1/2}\{(f+\hat{f}\delta_{\alpha z})\tfrac{1}{2}[d^-_\alpha(s)+d^+_\alpha(s+n-1)]+F_\alpha(\theta)\}$$
$$=-(f+\tfrac{1}{3}\hat{f})\left\{(\delta_{jA}-\delta_{jB})\frac{1}{2}\left[\frac{1-c_j(s)}{M_jM_C}\right]^{1/2}h_\alpha(s|\theta)+\left[\frac{c_A(s)c_B(s)}{M_AM_B}\right]^{1/2}[\delta_{jA}e_{B\alpha}(s1|\theta)+\delta_{jB}e_{A\alpha}(s1|\theta)]\right\}, \tag{19}$$

$$\left[\omega^2-\frac{1}{M_C}(f+\tfrac{1}{3}\hat{f})\right]h_\alpha(s|\theta)=-\tfrac{1}{2}(f+\tfrac{1}{3}\hat{f})\frac{1}{(M_C)^{1/2}}\left\{\left[\frac{x_s}{M_A}\right]^{1/2}e_{A\alpha}(s1|\theta)-\left[\frac{1-x_s}{M_B}\right]^{1/2}e_{B\alpha}(s1|\theta)\right\},$$

where an average $h_\alpha(s|\theta)$ of the correlation functions over the four nearest neighbors, right-hand and left-hand dipole moments $d^\pm_\alpha(s|\theta)$ of the sth molecule layer, and the vector components $F_\alpha(\theta)$ of the long-range electric forces related to the total dipole moment of the superlattice elementary cell are defined as

$$h_\alpha(s|\theta)=\tfrac{1}{4}\sum_{i=1}^{4}h_{A\alpha}(si|\theta)=-\tfrac{1}{4}\sum_{i=1}^{4}h_{B\alpha}(si|\theta)\ ,$$
$$d^\pm_\alpha(s|\theta)=\left[\frac{1-x_s}{M_A}\right]^{1/2}e_{A\alpha}(s1|\theta)+\left[\frac{x_s}{M_B}\right]^{1/2}e_{B\alpha}(s1|\theta)-\frac{1}{(M_C)^{1/2}}e_{C\alpha}\left[s-\frac{1\pm1}{2}2|\theta\right], \tag{20}$$
$$F_\alpha(\theta)=\hat{f}\sum_{\alpha'}A_{\alpha\alpha'}(\theta)\frac{1}{N}\sum_{s=1}^{N}d^-_{\alpha'}(s|\theta)\ .$$

In Eq. (19) the coupling of different vibration directions $\alpha=x,y,z$ is due to the long-range electric-field forces $F_\alpha(\theta)$. The equation for the fluctuation correlations $h_\alpha(s|\theta)$ does not give rise to additional complications. Together with the second equation for sublattice 1 it only increases the number of superlattice modes. However, the classification of these modes is the same as in pure $(GaAs)_{N_1}(AlAs)_{N_2}(001)$ superlattices ($N_1+N_2=N$).[38,42] One observes symmetric and antisymmetric s-polarized phonons with atomic displacements in the x direction and $F_x(\theta)=0$ by definition (18). In the case of p polarization the long-range electric force components $F_{y/z}(\theta)$ vanish for antisymmetric modes. That means the atomic displacements in the y and z direction remain decoupled in this case. For p-polarized symmetric modes the electric forces $F_{y/z}(\theta)$ only vanish for propagation parallel to the growth axis, i.e., $\theta=0$. In this complicated case a system of $8N$ equations (19) has to be solved for a given propagation direction θ. In the other limits with $F_\alpha(\theta)=0$ the number of equations is only $4N$. In the following we restrict ourselves only on the simpler cases where $F_\alpha(\theta)=0$. That means, we consider all s-polarized phonons and all p-polarized antisymmetric vibrations without restriction to the propagation direction. From all p-polarized symmetric modes only those propagating parallel to the growth direction are taken into account.

The pronounced influence of the composition profile x_s within the superlattice elementary cell and the disorder produces not only a doubling of the number of Eqs. (19) but also additional forces on the right-hand sides of the equations for the A and B atoms. These forces are proportional to correlations in fluctuations of sites in sublattice 1 and weighted atomic displacements. Another interesting point concerns the appearance of the Coulomb force constant $\hat{f}$ also in equations for phonons like the s-polarized ones that are usually not influenced by any elec-

tric field. However, this exactly happens in Eqs. (19) for mole fractions of the A and B atoms $c_j(s)<1$. Then, as an effect of the alloying, additional short-range forces $\sim(f+\frac{1}{3}\hat{f})$ occur. In the bulk alloy case they bring the frequencies of the impurity modes from the transverse and the longitudinal problem together in the dilute limits.

Labeling the eigenmodes of the system of Eqs. (19) with eigenfrequencies $\omega_\lambda(\theta)$ by the index λ ($\lambda=1,\ldots,12N$), the wave-vector-resolved (more strictly here angle-resolved) one-phonon density of states $D(\omega,\theta)$ can be expressed by the spectral weights g_λ according to ($\omega>0$),

$$D(\omega,\theta)=\frac{1}{6N}\sum_{\lambda=1}^{12N}2\omega\delta(\omega^2-\omega_\lambda^2(\theta))g_\lambda(\theta)\ , \tag{21}$$

with

$$g_\lambda(\theta)=\sum_{\alpha,s,n}|G_\alpha^\lambda(sn,\theta)|^2\ , \tag{22}$$

$$G_\alpha^\lambda(sn,\theta)=\left[\frac{\omega_\lambda(\theta)}{\hbar}\right]^{1/2}\sum_j[c_j(s)]^{1/2}e_{j\alpha}^\lambda(sn\,|\theta)\ . \tag{23}$$

In contrast to modes for a given ideal configuration, where it holds that $g_\lambda=1$ in correspondence to the orthonormalization and completeness of the $6N$ modes, the spectral weights of the $12N$ eigenmodes of the averaged system fulfill the condition $0<g_\lambda<1$.

IV. DISCUSSION

A. Vibrational modes in compositionally disordered superlattices

For simplicity we start the discussion with the most short-period $(A_{1-x_1}B_{x_1}C)_1(A_{1-x_2}B_{x_2}C)_1(001)$ superlattice with two molecule layers $s=1,2$ and a certain concentration profile expressed by the two Al mole fractions x_1 and x_2. Even in the case $F_\alpha(\theta)\equiv0$ under consideration the three identical 8×8 eigenvalue problems (19) for each $\alpha=x,y,z$ are not analytically solvable in contrast to the case without alloy effects.[38] Analytical solutions can be obtained in the dilute limits $x_1=0$, $x_2=1$, and $x_1=1$ and $x_2=0$. For each polarization direction and displacement direction α, respectively, one derives four superlattice modes

$$\begin{aligned}
&\omega^2=0\ ,\\
&\omega^2=(f+\hat{f}\delta_{\alpha z})/M_C\ ,\\
&\omega_\pm^2=\tfrac{1}{2}(f+\hat{f}\delta_{\alpha z})\left\{\frac{1}{M_A}+\frac{1}{M_B}+\frac{1}{M_C}\right.\\
&\qquad\left.\pm\left[\frac{1}{M_C^2}+\left[\frac{1}{M_B}-\frac{1}{M_A}\right]^2\right]^{1/2}\right\}.
\end{aligned} \tag{24}$$

They are the acoustic mode, the acoustic mode folded from the bulk X point to the Γ point in the superlattice elementary cell, and the AC-like as well as the BC-like confined optical modes. The four additional solutions describe impurity modes ($j=A,B$)

$$\omega_{j\pm}^2=\tfrac{1}{2}(f+\tfrac{1}{3}\hat{f})\left\{\frac{1}{M_j}+\frac{1}{M_C}\right.$$
$$\left.\pm\left[\frac{1}{M_jM_C}+\left[\frac{1}{M_j}-\frac{1}{M_C}\right]^2\right]^{1/2}\right\}. \tag{25}$$

They are independent of polarization and displacement direction α. The $\omega_{A\pm}$ modes are impurity modes in the alloy $A_{1-x}B_xC$ in the dilute limit $x\to1$. The $\omega_{B\pm}$ vibrations describe such modes for $x\to0$. The occurrence of the doublet $\omega_{j\pm}$ is a consequence of two additional equations per effective molecule. ω_{j+} denotes the frequencies of the conventional impurity modes in the optical-phonon region. In both cases $M_A<M_B<M_C$ and $M_B<M_A<M_C$ ω_{j+} ($j=A,B$) describe gap modes in agreement with the findings for alloys.[36] The low-frequency roots ω_{j-} represent disorder-activated acoustic modes.[26,36]

For $\alpha=z$ and a $(GaAs)_1(Ga_{1-x}Al_xAs)_1(001)$ superlattice a complete frequency spectrum ω_λ is shown in Fig. 1. The accompanying spectral weights g_λ are plotted in Fig. 2 versus the Al mole fraction x. Parameters are taken from Ref. 38. Since $x_1=0$ is assumed from the very beginning the corresponding impurity modes with zero spectral weights are not represented in Figs. 1 and 2. For AlAs-barrier layers, i.e., $x=1$, one observes the modes discussed above, four superlattice modes, and the two GaAs-like impurity phonons with zero spectral weight. The acoustic phonon and the folded acoustic modes are partially not influenced by the Al mole fraction x. The

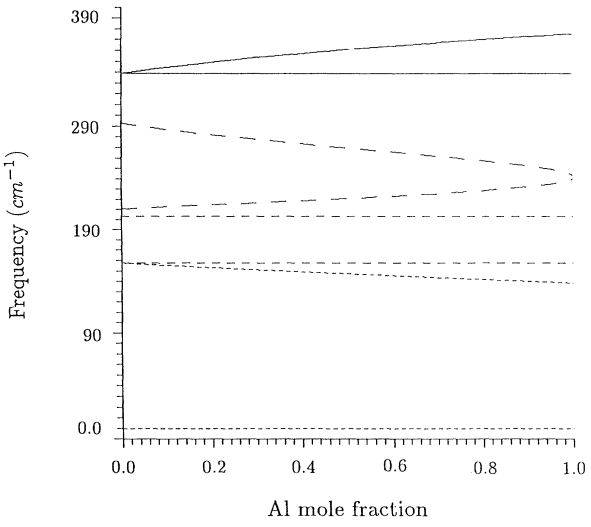

FIG. 1. Zone-center frequencies of vibrations parallel to the growth axis of a $(GaAs)_1(Ga_{1-x}Al_xAs)_1(001)$ superlattice with vanishing long-range electric forces vs the composition of the barrier layers derived from the generalized REI model. The impurity modes with zero spectral weights are dropped.

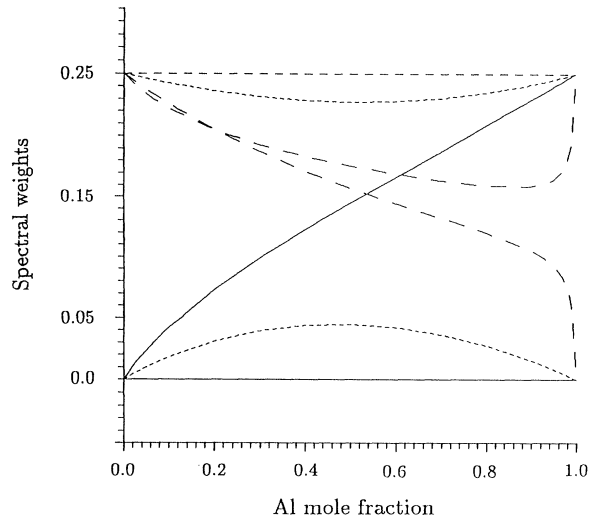

FIG. 2. Spectral weights of the modes shown in Fig. 1.

strongest influence of the decreasing composition x concerns the optical phonons. The intensity of the AlAs-like optical phonon decreases with decreasing x. Simultaneously the peak splits. A second maximum closer to the frequency of the AlAs-like impurity mode in GaAs appears. The GaAs-like optical phonon shifts to higher frequencies towards the position of the LO(Γ) phonon of the bulk. Because of its near-energy overlap with the disorder-activated mode it loses its confined character relatively fast. Analogously the disorder-activated vibrations change over into a GaAs-like LO(X) phonon folded to the Γ point of the superlattice elementary cell.

All these features we recognize in the density of states of the Γ phonons. The corresponding Fig. 3 is calculated by the mentioned completely stochastic model realized by random configurations in supercells. Supercells containing 7200 atomic sites and a numerical Lorentzian line

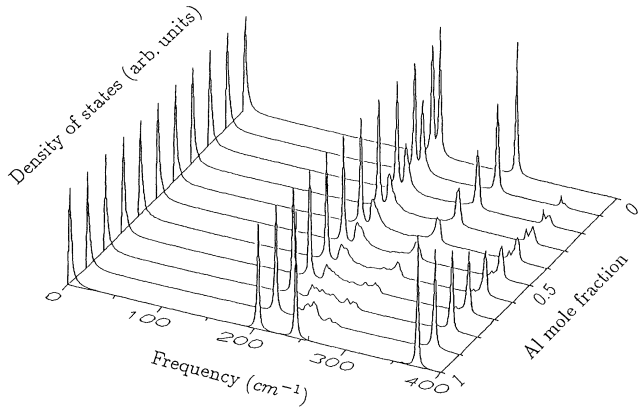

FIG. 3. Density of states of the phonons shown in Fig. 1. Results are obtained from a stochastic model using supercells with 7200 atoms.

broadening of 1 cm^{-1} are chosen. Only one effective force constant $f+\hat{f}$ reproducing the LO(Γ) phonon of GaAs (Ref. 38) is taken into account. The full numerical model and the generalized REI model give rise to nearly the same results with respect to peak positions and spectral weights of the peaks. There are two failures of the REI approach. The variety of disorder-activated peaks in the optical frequency region of GaAs above the LA(X) phonon and the disorder-induced broadening cannot be reproduced. As expected the REI model fails in parameter regions where the well-dispersive character, more strictly speaking bandlike character, of the phonon modes is destroyed. In all other cases the results obtained are sufficient.

B. Influence of barrier composition: Confinement versus folding

To discuss the influence of the Al content in the barrier material of a $(GaAs)_{N_1}(Ga_{1-x}Al_xAs)_{N_2}(001)$ superlattice with $N_1=N_2=N/2$ we study superlattices with thicker layers as in the 1×1 case. A certain optimum with respect to layer thickness and calculation effort corresponds to $N_1=N_2=4$. Results for the density of states and the same parameter constellation as used in Figs. 1–3 are plotted in Fig. 4 for different compositions x. The uninteresting acoustic-phonon region below 200 cm^{-1} is cut.

The REI model and the supercell method with 28 800 atomic sites per cell are applied. The quality of the REI model with respect to the full stochastic model discussed already in the 1×1 case is confirmed by Fig. 4. Peak positions and number of peaks are reproduced within the REI model in a reasonable manner. The most pronounced failure of the generalized REI approach concerns the disorder-induced broadening effects which, however, are of different importance in dependence on the Al mole fraction and the spectral region.

Apart from the disorder-induced line broadening we expect three effects of the varying composition in the barrier layers of the superlattice: (i) shift of frequencies, (ii) variation of the depth of the quantum wells for the AlAs-like and GaAs-like confined optical phonons, and (iii) decrease of AlAs-related peaks and increase of GaAs-related maxima with decreasing Al mole fraction. In fact, all these effects appear in Fig. 4 representing Γ phonons with vanishing accompanying electric fields. In the ordered case, $x=1$, we observe only the well-known four confined LOn phonons in the GaAs and AlAs frequency region. The four AlAs-like LOn phonons remain stable in a wide x range. That means the four peaks are visible although they are broadened by disorder effects. Their intensities decrease in accordance with x. Lower than about $x=0.2$ only a broad impurity band with vanishing intensity appears. On the other hand, the GaAs-like optical phonons exhibit a completely different behavior. LO1 and in a wide range also LO2 are hardly influenced by the decrease of the Al mole fraction x in the barrier material. That means that although its depth decreases the quantum well remains important for these phonons. The transition from the confined character to that of folded phonons happens rather rapidly for small

x. On the other hand, the LOn phonons lower in frequency are much more influenced by disorder in agreement with the higher number of nodes in the displacement pattern and their weaker localization.[38] The most pronounced changes occur in the frequency region around LO3. Beside the disorder-activated features this fact is governed by the existence of a second GaAs-like LO-phonon band being lower in energy and localized in the alloy.

In the limit $x \rightarrow 0$ five GaAs-like optical peaks remain in the spectrum as a result of the folding effect. Since there is no difference in the two GaAs layers of the $(GaAs)_4(GaAs)_4(001)$ superlattices the three central peaks are twofold degenerated. This fact is indicated in the density of states by the peak intensity. It should be noted that a confined-to-propagating transition of LO phonons in $GaAs/Ga_{1-x}Al_xAs$ superlattices is observed by time-resolved Raman scattering for relatively thick GaAs layers.[19]

The localization behavior of the different GaAs-like modes and the transition from the confined character to folded phonons is demonstrated in more detail in Fig. 5. It represents the displacement pattern of the eight As atoms in the superlattice elementary cell in dependence on the Al content in the alloy forming the barrier layers. Following the situations from $x=1$ to 0 the transitions of the two confined phonons with one or four nodes into folded bulk phonons arising from the zone center Γ or the zone boundary X is clearly visible. Thereby, this transition happens for concentrations x closer to 1 in the case of LO4 compared to LO1, where the transition occurs near $x=0$. The reason is the energy overlap of GaAs-like modes of the alloy and of GaAs.[44]

C. Influence of interface broadening

To study the effect of interface broadening due to cation interdiffusion we solve the lattice-dynamical problem for superlattices with four or more material layers within the superlattice elementary cell. For systems thicker than $N=2$ the possibility of two differently disordered interfaces exists in the $(GaAs)_{N_1}(AlAs)_{N_2}$ systems $(N_1+N_2=N)$. Therefore the experimentally well-established fact of the asymmetric growth at the

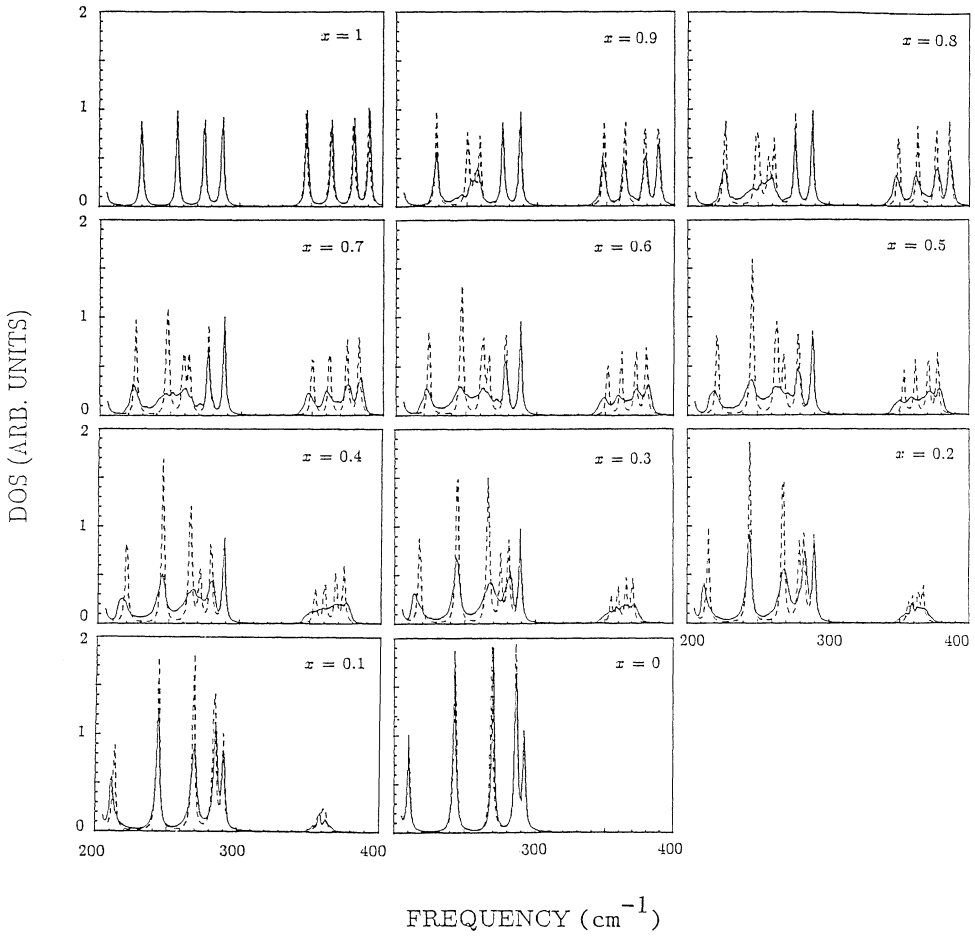

FIG. 4. Density of states of the zone-center optical phonons of a $(GaAs)_4(Ga_{1-x}Al_xAs)_4(001)$ superlattice with displacements parallel to the growth direction and vanishing long-range electric forces $F_z(\theta)$. Results of a completely stochastic model with 28 800 atomic sites per supercell (solid lines) are compared with those from the generalized REI model (dashed lines).

AlAs/GaAs and GaAs/AlAs interfaces in the GaAs/AlAs samples[45] can be taken into account. We do this assuming completely different concentration profiles for the two interfaces per elementary cell. We start from an abrupt interface and a second one where the interface broadening is restricted to one cation layer at each side of the As layer centered in the nominal interface. The problem can be modeled by a

$$(\mathrm{GaAs})_{N_1-1}(\mathrm{Ga}_{1-x}\mathrm{Al}_x\mathrm{As})_1(\mathrm{Ga}_x\mathrm{Al}_{1-x}\mathrm{As})_1(\mathrm{AlAs})_{N_2-1}(001)$$

superlattice. The composition $x=0$ describes sharp interfaces whereas a composition $x=0.5$ stands for a complete alloying of the interface region. As in the last section we restrict ourselves to an $N_1=N_2=4$ short-period superlattice. The corresponding density of states for zone-center optical phonons is derived from the fully stochastic model including one effective force constant $f+\hat{f}$, which is fitted to reproduce the bulk zone-center LO phonon of GaAs, and more than 20 000 atoms per supercell. It is plotted in Fig. 6.

The spectrum for $x=0$ shows again the four AlAs-like and the GaAs-like confined LOn phonons. The peak somewhat above 200 cm^{-1} represents the bulk LA(X) phonon folded onto the Γ point of the superlattice Brillouin zone. It is able to guide the eye since it is practically not influenced by the interface broadening. Despite the presence of interface broadening for $x=0.1,\ldots,0.5$ the AlAs-like and GaAs-like LO1 and LO4 phonons remain rather stable. This holds particularly for the LO1 phonons. As we discuss below, they exhibit a small downshift in the frequencies. Additionally their intensity somewhat decreases in agreement with the fact that the effective layer thickness affecting this phonon decreases. Furthermore, the LO4 modes underly a remarkable interface-disorder-induced line-shape broadening. On the other hand, the LO3 and especially the LO4 phonons are drastically influenced by the interface profile. Apart

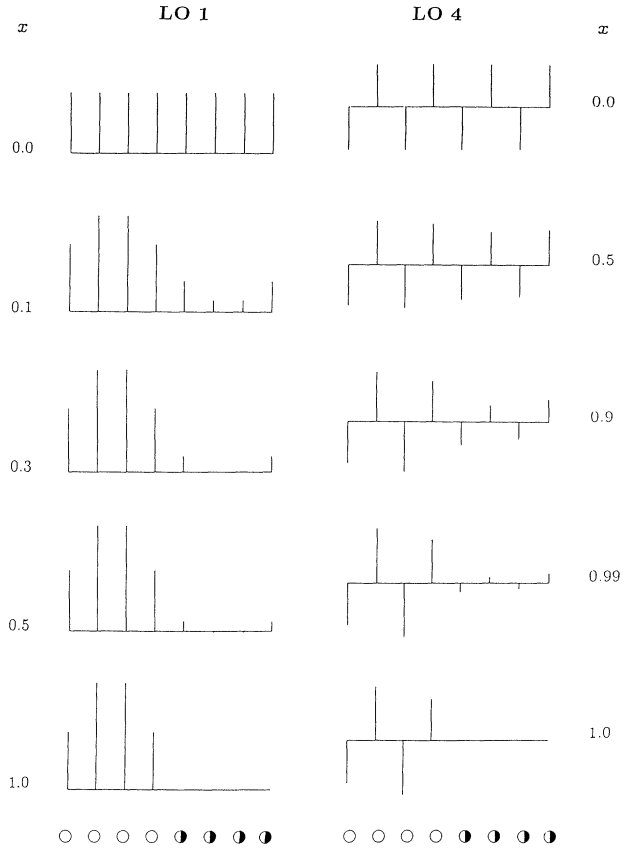

FIG. 5. Displacements of the As atoms parallel to the growth directions for GaAs-like LO1 and LO4 phonons in a $(\mathrm{GaAs})_4(\mathrm{Ga}_{1-x}\mathrm{Al}_x\mathrm{As})_4(001)$ superlattice. Equilibrium positions of As atoms in GaAs and the alloy are indicated by circles and half-filled dots.

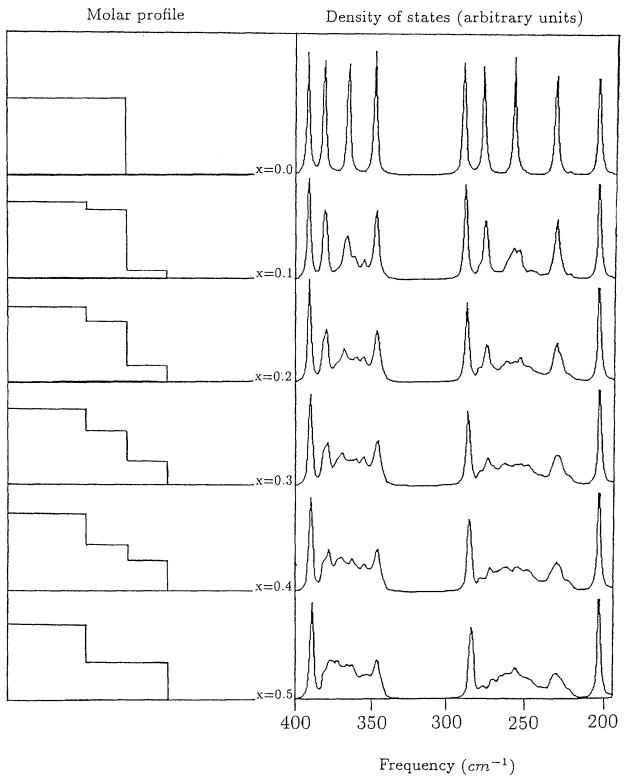

FIG. 6. Density of states of zone-center phonon-related atomic displacements in the z direction but not accompanied by the long-range electric field for $(\mathrm{GaAs})_3(\mathrm{Ga}_{1-x}\mathrm{Al}_x\mathrm{As})_1(\mathrm{Ga}_x\mathrm{Al}_{1-x}\mathrm{As})_1(\mathrm{AlAs})(001)$ superlattices. The fully stochastic model with effective force constant is applied. The degree of cation interdiffusion at the interface is changed (cf. left panel).

from line-shape broadening effects the main reason seems to be caused by the appearance of additional peaks related to phonons with frequencies close to those in the $Ga_{1-x}Al_xAs$ and $Ga_xAl_{1-x}As$ alloys and in the corresponding 1×1 superlattices, respectively.

The downshift of the LO1 frequency discussed above is represented in more detail in Fig. 7 versus the total number N of molecule layers within the superlattice elementary cell. The frequencies are calculated for phonon propagation parallel to the superlattice axis within the framework of the generalized REI model in Eqs. (19) and pure mass disorder. Three different situations (a)–(c) of interface disorder are considered. In Fig. 7(a) only one interface is assumed to be interdiffused. Again ($N \geq 4$)

$$(Ga_{1-y}Al_yAs)_1(GaAs)_{N/2-2}(Ga_{1-x}Al_xAs)_1(Ga_xAl_{1-x}As)_1(AlAs)_{N/2-2}(Ga_yAl_{1-y}As)_1(001)$$

superlattices are considered. In Fig. 7(b) one interface is assumed to be completely intermixed ($y=0.5$), whereas the other one is more abrupt, i.e., $x=0,\ldots,0.5$. In Fig. 7(c) the situation where both interfaces show the same degree of cation interdiffusion is represented. The calculated frequencies are far from agreement with the position of the LO1 phonons in Raman spectra. The simple force-constant model and the assumption of pure mass

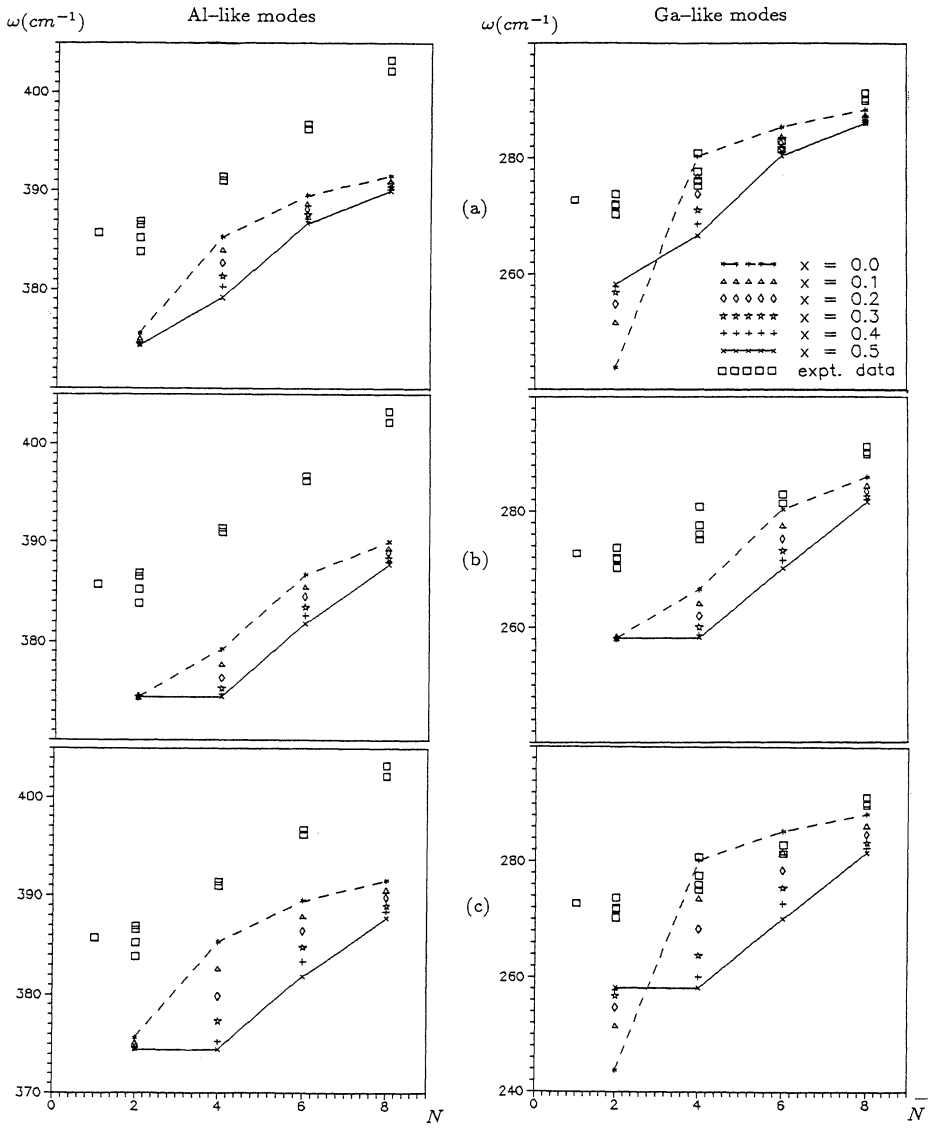

FIG. 7. AlAs-like and GaAs-like LO1 phonon frequencies of a $(Ga_{1-y}Al_yAs)_1(GaAs)_{N/2-2}(Ga_{1-x}Al_xAs)_1(Ga_xAl_{1-x}As)_1(AlAs)_{N/2-2}(Ga_yAl_{1-y}As)_1(001)$ superlattice are plotted vs the total number N of molecule layers in an elementary cell. Results for different degrees of interface broadening calculated within the generalized REI model are shown. The squares correspond to Raman data collected in Ref. 14. The points at $N=1$ indicate the corresponding alloy frequencies. (a) $y=0$, (b) $y=0.5$, and (c) $y=x$.

disorder can only nearly fit the bulk GaAs-LO frequency. For AlAs our results are always lower in frequency since the smaller ion charge of GaAs is applied. Nevertheless, the calculated frequencies are helpful to discuss the dependence on the number of molecule layers in the elementary cell and the influence of interface intermixing. This is especially true for the GaAs-like modes. Abrupt interfaces give rise to a considerable downshift of the frequency going from the 2×2 superlattice to the 1×1 superlattice. This effect is not observed in experiment. Raman scattering predicts a more smooth transition ending with a LO1 frequency of the 1×1 superlattice close to the corresponding LO frequency of the alloy. As in more sophisticated theories[12,14] this effect can also be traced back to interface broadening due to cation interdiffusion in the extended REI model. The comparison of Figs. 7(a), 7(b), and 7(c) shows that the details of this transition depend on the actual behavior of the two interfaces GaAs/AlAs and AlAs/GaAs within one superlattice elementary cell.

The more physical reasons for the weaker or stronger frequency shift can be seen from Fig. 8 where the displacement fields of the As atoms in z direction are plotted for the GaAs-like LO1 mode for different degrees of interface disorder. Although only extreme short-period superlattices are considered in Fig. 8 drastic differences for different numbers of molecule layers N are observed. Introducing one disordered interface influencing two molecule layers the quantum well for the GaAs-like LO1 phonon reduces its effective thickness by $a_0/2$, the thickness of one molecule layer (cf. Fig. 8). The confinement is increased, resulting in a downshift of the mode frequency. The intermixing parameter x characterizes the height of the asymmetric quantum well on the side of the graded interface. With rising x this height proportional to the frequency difference of the GaAs-like LO mode in GaAs and $Ga_{1-x}Al_xAs$ in increased, which also enforces the confinement. Another interesting point concerns the visible asymmetry of the mode patterns. This can influence the Raman selection rules for short-period superlattices.

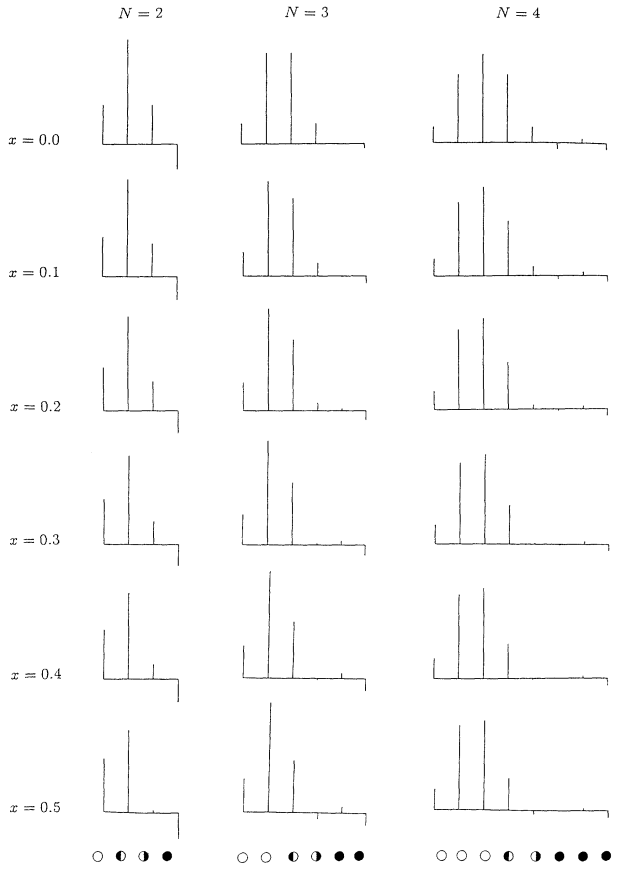

FIG. 8. Patterns of anion displacements in z direction for the GaAs-like LO1 phonon propagating with zero wave vector parallel to the growth direction of $(GaAs)_{N/2-1}(Ga_{1-x}Al_xAs)_1(Ga_xAl_{1-x}As)_1(AlAs)_{N/2-1}(001)$ superlattices with different x. The positions of the As atoms are indicated by circles in GaAs and dots in AlAs in the case $x=0$.

V. SUMMARY

We have introduced a model for phonon modes in layered structures on the basis of the ternary material system $A_{1-x}B_xC$ grown in an arbitrary direction and representing any concentration profile x_m over all atomic layers perpendicular to the growth direction. The lattice-dynamical problem is solved starting from the configurationally averaged equations of motion of the atoms in the system. The hierarchy of equations is decoupled by restricting the correlations between fluctuations in the occupation of the A or B sites and the composition-induced fluctuations of the displacements of C atoms to nearest neighbors. For $A_{1-x}B_xC$ alloy systems with well-defined dispersive character of the phonons independently of one- or two-mode behavior the right-hand side of the equation of motion for this correlation function is traced back to averaged displacement fields and the correlation function itself by means of a one-site approximation. One obtains a generalized REI model. It is applicable to arbitrary layered systems with compositional disorder and to all phonons of the system. No additional force constants not included already in the bulk problems are introduced. The impurity force constant of the conventional REI model is determined from the equations of motion for the correlation functions.

The theory is applied to (001) superlattices with a certain composition profile x_s in the superlattice elementary cell. To simplify the equations of motion we specify the dynamical matrix to the case of pure mass disorder and the Born-Huang model. These specifications seem to give a reasonable description of long-wavelength optical phonons in superlattices manufactured from $Ga_{1-x}Al_xAs$ ternary compounds. The solutions of the lattice-dynamical equations within the generalized REI model are taken to discuss the wave-vector-resolved density of states, the frequencies, and the displacement patterns.

The density of states is compared with results of a completely stochastic model describing the configuration average by taking into account sufficiently large supercells. We find that the generalized REI model gives reasonable results. Only in a few cases, when, for instance, the disorder-induced broadening is too strong or the energy overlap between GaAs-like phonons in GaAs and $Ga_{1-x}Al_xAs$ is remarkable, do more sophisticated theoretical descriptions have to be applied. Explicitly we discuss two interesting cases: First, the transition from the confined to the folded behavior of optical phonons with the Al mole fraction x in $(GaAs)_{N/2}(Ga_{1-x}Al_xAs)_{N/2}(001)$ superlattices; second, the effect of broadening of one of the two interfaces in a nominal $(GaAs)_{N/2}(AlAs)_{N/2}(001)$ superlattice due to cation interdiffusion is studied in the case of density of states, frequencies, and displacements.

ACKNOWLEDGMENTS

We are grateful to P. Kleinert, S. R. P. Smith, and J. Spitzer for useful discussions. This work was supported by a Research Grant of the Deutsche Forschungsgemeinschaft under Grant No. Be 1346/2-1.

[1]B. Jusserand and M. Cardona, in *Light Scattering in Solids V, Superlattices and Other Microstructures,* edited by M. Cardona and G. Güntherodt (Springer-Verlag, Berlin, 1989), p. 49, and references therein.
[2]J. Menendez, J. Lumin. **44**, 285 (1989).
[3]A. Fasolino and E. Molinari, Surf. Sci. **228**, 112 (1990).
[4]S. Baroni, P. Giannozzi, and A. Resta, Phys. Rev. Lett. **58**, 1861 (1987).
[5]S. Baroni, P. Giannozzi, and E. Molinari, Phys. Rev. B **41**, 3870 (1990).
[6]M. Cardona, T. Suemoto, N. E. Christensen, T. Isu, and K. Ploog, Phys. Rev. B **36**, 5906 (1987).
[7]A. Ishibashi, M. Itabashi, Y. Mori, K. Kawado, and N. Watanabe, Phys. Rev. B **33**, 2887 (1986).
[8]M. Nakayama, K. Kubota, H. Kato, S. Chika, and N. Sano, Solid State Commun. **53**, 493 (1985).
[9]T. Toriyama, N. Kobayashi, and Y. Horikoshi, Jpn. J. Appl. Phys. **25**, 1895 (1986).
[10]G. Fasol, M. Tanaka, H. Sakaki, and Y. Horikoshi, Phys. Rev. B **38**, 6056 (1988).
[11]B. Jusserand, Phys. Rev. B **42**, 7265 (1990).
[12]D. Kechrakos, P. R. Briddon, and J. C. Inkson, Phys. Rev. B **44**, 9114 (1991).
[13]B. Samson, S. R. P. Smith, C. T. Foxon, D. Hilton, and K. J. Moore, Solid State Commun. **78**, 325 (1991); B. Samson, T. Dumelow, A. A. Hamilton, T. J. Parker, S. R. P. Smith, D. R. Tilley, C. T. Foxon, D. Hilton, and K. J. Moore, Phys. Rev. B **46**, 2375 (1992).
[14]E. Molinari, S. Baroni, P. Giannozzi, and S. de Gironcoli, Phys. Rev. B **45**, 4280 (1992).
[15]G. Scamarcio, L. Tapfer, W. Konig, A. Fischer, K. Ploog, E. Molinari, S. Baroni, P. Giannozzi, and S. de Gironcoli, Phys. Rev. B **43**, 14 754 (1991).
[16]A. K. Sood, J. Menendez, M. Cardona, and K. Ploog, Phys. Rev. Lett. **54**, 2111 (1985).
[17]B. Jusserand and D. Paquet, Phys. Rev. Lett. **56**, 1752 (1986).
[18]E. Molinari, A. Fasolino, and K. Kunc, Superlatt. Microstruct. **2**, 397 (1986).
[19]D. S. Kim, A. Bouchalkha, J. M. Jacob, J. F. Zhou, J. J. Song, and J. F. Klemm, Phys. Rev. Lett. **68**, 1002 (1992).
[20]B. Jusserand, D. Paquet, and F. Mollot, Phys. Rev. Lett. **63**, 2397 (1989).
[21]Y. S. Chen, W. Shockley, and G. L. Pearson, Phys. Rev. **151**, 648 (1968).
[22]A. S. Barker and A. J. Sievers, Rev. Mod. Phys. **47**, Suppl. 2, S1 (1975).
[23]K. Kunc and H. Bilz, Solid State Commun. **19**, 1927 (1976).
[24]A. S. Barker, Jr., J. L. Merz, and A. C. Gossard, Phys. Rev. B **17**, 3181 (1978).
[25]O. K. Kim and W. G. Spitzer, J. Appl. Phys. **50**, 4362 (1979).
[26]R. Bonneville, Phys. Rev. B **29**, 907 (1984).
[27]S. Baroni, S. de Gironcoli, and P. Giannozzi, Phys. Rev. Lett. **65**, 84 (1990).
[28]B. Jusserand, F. Alexandre, D. Paquet, and G. LeRoux, Appl. Phys. Lett. **47**, 301 (1985).
[29]B. Jusserand, F. Mollot, L. G. Quagliano, G. LeRoux, and R. Planel, Phys. Rev. Lett. **67**, 2803 (1991).
[30]S. Baroni, P. Pavone, P. Giannozzi, S. de Gironcoli, and E. Molinari (unpublished).
[31]L. Miglio, C. Molteni, and M. Bernasconi, Appl. Phys. Lett. **59**, 788 (1991); C. Molteni, L. Colombo, L. Miglio, G. Benedek, and M. Bernasconi, Philos. Mag. B **65**, 325 (1992).
[32]J. A. Kash, J. M. Hvam, J. C. Tsang, and T. F. Kuech, Phys. Rev. B **38**, 5776 (1988).
[33]I. F. Chang and S. S. Mitra, Phys. Rev. **172**, 924 (1968); Phys. Rev. B **2**, 1215 (1980); Adv. Phys. **20**, 359 (1971).
[34]X. Wang and X. X. Liang, Phys. Rev. B **42**, 8915 (1990).
[35]H. Gerecke, H. Grille, and F. Bechstedt, Verh. Dtsch. Phys. Ges. (VI) **27**, 594 (1992); Superlatt. Microstruct. **12**, 463 (1992).
[36]H. Böttger, *Principles of the Theory of Lattice Dynamics* (Akademie-Verlag, Berlin, 1983).
[37]M. Born and K. Huang, *Dynamical Theory of Crystal Lattices* (Clarendon, Oxford, 1954).
[38]F. Bechstedt and H. Gerecke, Phys. Status Solidi B **154**, 565 (1989).
[39]H. Gerecke, Ph.D. thesis, Friedrich-Schiller-Universität, Jena, 1991.
[40]W. Cochran and R. A. Cowley, J. Chem. Phys. Solids **23**, 447 (1962).
[41]H. Chu, S.-F. Ren, and Y.-C. Chang, Phys. Rev. B **37**, 10 746 (1988).
[42]F. Bechstedt and H. Gerecke, Phys. Status Solidi B **156**, 151 (1989); J. Phys. Condens. Matter **2**, 4363 (1990).
[43]H. Gerecke and F. Bechstedt, Phys. Rev. B **43**, 7053 (1991).
[44]A. Kobayashi and R. Roy, Phys. Rev. B **35**, 2237 (1987).
[45]M. Tanaka, H. Ichinose, T. Furuta, Y. Ishida, and H. Sakaki, J. Phys. (Paris) Colloq. **47**, C5-101 (1987).